JAERI-M
83-017

PREPARATORY EVALUATION ON HEAT AND PARTICLE LOADS, HELIUM PUMPING, AND LIMITER MATERIAL FOR INTOR PUMPED LIMITER

February 1983

Seiji SAITO*, Noboru FUJISAWA, Masayoshi SUGIHARA
Koju UEDA** and Hiroo NAKAMURA

日本原子力研究所
Japan Atomic Energy Research Institute

JAERI-Mレポートは，日本原子力研究所が不定期に公刊している研究報告書です。
入手の問合わせは，日本原子力研究所技術情報部情報資料課（〒319-11茨城県那珂郡東海村）あて，お申しこしください。なお，このほかに財団法人原子力弘済会資料センター（〒319-11 茨城県那珂郡東海村日本原子力研究所内）で複写による実費頒布をおこなっております。

JAERI-M reports are issued irregularly.
Inquiries about availability of the reports should be addressed to Information Section, Division of Technical Information, Japan Atomic Energy Research Institute, Tokai-mura, Naka-gun, Ibaraki-ken 319-11, Japan.

編集兼発行　日本原子力研究所
印　　刷　㈱高野高速印刷

Preparatory Evaluation on Heat and Particle Loads, Helium Pumping, and Limiter Material for INTOR Pumped Limiter

Seiji SAITO*, Noboru FUJISAWA, Masayoshi SUGIHARA
Koju UEDA** and Hiroo NAKAMURA

Division of Large Tokamak Development, Tokai Research Establishment, JAERI

(Received January 27, 1983)

Toroidal belt-type pumped limiters are discussed as a possible method for the heat removal and helium ash exhaust in INTOR. The comparisons are made between two typical configurations of the pumped limiter from the various viewpoints: the heat and particle fluxes, pumping speed, sputtering erosion and impurity accumulation in main plasma. In the first configuration, the limiter plate is set up tangential to the outer most plasma surface. In the second configuration, the limiter plate is inserted near the null point of the poloidal magnetic field. It is found that the both types of the pumped limiters suffer nearly the same various conditions from overall aspects.

Keywords: INTOR, Pumped Limiter, Heat Removal, Helium Ash, Material Pumping Speed, Sputtering, Erosion, Poloidal Field

---

* On leave from Hitachi, Ltd.

** On leave from Mitsubishi Electric Co.

INTOR 装置におけるポンプリミタに対する熱および粒子負荷，必要排気速度あるいはリミタ材料の予備的検討

日本原子力研究所東海研究所大型トカマク開発部
斉藤誠次*・藤沢　登・杉原正芳・上田孝寿**・中村博雄

（１９８３年１月２７日）

INTOR 装置において，ＤＴ反応により生じる熱およびヘリウムの除去方法の一つとして，トロイダルポンプリミタを検討した。ここでは，INTOR 装置で代表的と考えられる２種のリミタ配置を対象に，リミタ面上の熱負荷および粒子負荷，あるいは排気系に必要とされる排気速度等の評価から両者を比較検討した。また，スパタリングによるリミタ材の損耗率およびプラズマ中の不純物混入量の評価からリミタ材料の選定を行った。第一は，プラズマ外周の磁気面に接するように，リミタ板を配置する方式であり，第二はポロイダル磁場のヌル点上にリミタ板を挿入する方式である。両者ともに全体的にほぼ同等の条件のもとで実現可能であることがわかった。

＊　外来研究員：（株）日立製作所
＊＊　外来研究員：三菱電機

Contents

目　　次

1. Introduction

In INTOR Phase One workshop, which completed its conceptual design in July 1981, the poloidal divertor concept was adopted for impurity control including ash exhaust, and its workable design was developed[1]. Successively, the INTOR workshop entered into the Phase IIA. In that phase, the poloidal divertor is being studied in more depth, and at the same time, the pumped limiter concept supplemented with some impurity control schemes was adopted as a desirable impurity control measure from the viewpoint of its structual simplicity and its possible reduction in the device size[2].

The pumped limiter has the following features compared with the poloidal divertor:

(1) reduction in the reactor size as a result of the decrease or removal of the divertor region

(2) structural simplicity of the pumped limiter,

(3) reduction in poloidal coil power supply stemmed from the above compactness and simplicity of the device with the pumped limiter, which in turn results in the decreased forces on the toroidal coils, and it also reflects the further compactness of the device,

(4) need for supplementary impurity control for the pumped limiter concept, which has no active impurity control mechanism like the so-called divertor effect, except for the impurity screening effect in the scrape-off layer.

In this report, two type of limiters are proposed and their comparison is made. Next, plasma parameters in the scrape-off layer are evaluated, which lead to the specification of the profiles of heat and particle loads to the limiter, and the required pumping speed. Allowable

candidate limiter materials and their erosion rate are followed to be evaluated. Lastly, the sensitivity analysis of the heat and particle loads, and the pumping speed is presented for changes in the scrape-off parameters and the plasma major radius.

2. Two pumped limiter concepts

Two type of limiter configurations could be visualized from the difference in the scrape-off layer magnetic structure, One has no null-point in the plasma region including the scrape-off layer, and the limiter is located so as to be tangential to one of magnetic surfaces, which is the boundary between the main plasma and the scrape-off plasma, and helium ions in the outer scrape-off layer are neutralized on the back side of the limiter and are evacuated through the pumping duct, as shown in Fig. 1(a).

Another has the null point, and the plasma surface is defined by the separatrix, just like the poloidal divertor case. The limiters are placed in the vicinity of the null-point, as shown in Fig. 1(b). The helium ash could be exhausted using the tilt of the limiter. The former and the latter are called as T-type (Tangential type) and N-type (Null type), respectively.

The followings are preliminary qualitative comparisons between the N-type and the T-type pumped limiters from various viewpoints.

1) Heat and particle loads

Expansion of the heat and particle flux loads onto the limiters would be feasible in both cases, i.e. with small angle between the limiter surface and poloidal field lines in the T-type limiter, and with expansion of the scrape-off layer in the vicinity of the null-point in the N-type.

2) Space requirement

The expansion of the main plasma space due to the existence of the null-point leads to requirement of some larger space in the N-type limiter than the T-type.

3) Elongation

The T-type limiter configuration could not have large elongation, and 1.5-1.6 in elongation would be marginal, since the null-point approaches to the plasma surface in increasing elongation by the exterior poloidal coils to the toroidal coils.

4) Poloidal coil current

Larger poloidal coil current would be required in the N-type, because the null-point exists near the plasma surface.

5) Ash exhaust

Larger pumping speed would be needed in the N-type limiter, judging from the limiter configurations shown in Fig. 1.

6) Impurity control performance

Some divertor effect might be expected in the N-type limiter if the limiter was located a little away from the null-point.
The T-type limiter would require some another impurity controls in addition to the screening effect in the scrape-off plasma layer.

7) Accuracy in setting the limiters

High accuracy would be required in setting the T-type limiters along toroidal direction. Small errors in setting might cause the local concentration of the heat and particle fluxes. In the N-type, such a problem could be avoided, when the limiter is allocated a little away from the null-point.

8) Accuracy in magnetic field

This is the same as the above setting accuracy. For instance, in the T-type case, the toroidal field ripple might cause also the local concentration of the heat and particle loads.

9) Displacement of plasma

Some distance between the limiter surface and the null-point

could avoid some effect to the main plasma in the N-type limiter if plasma would shift vertically. On the other hand, the T-type limiter might need the accurate control of vertical position; otherwise, the main plasma parameters might change.

Judging from the above qualitative comparisons, some preference could be found in the N-type pumped limiter, although the N-type requires larger space, larger poloidal current, and larger pumping speed than the T-type limiter. The INTOR workshop resolved to forcus the initial limiter studies on the T-type limiter so as to clarify the important differences between the pumped limiter and divertor concepts, since the N-type limiter would have many features similar to the poloidal divertor.

3. Heat and particle flux distributions on limiter surface

Designing the pumped limiter configuration needs the heat and particle flux distributions on the limter surface, through which the transfered heat must be removed. It has been recognized by the analysis of heat removal from the divertor neutralizer plate that the maximum tolerable heat flux is less than 2 - 3 MW/m^2[3]. The above restriction forces the heat and particle fluxes flowing within the narrow region of the scrape-off plasma to expand on the limiter surface of the width about 1 m. The following evaluations on the scrape-off parameters will indicate that the permitted maximum heat load to the flat-type limiter is around 40 MW, when the maximum tolerable heat flux is limitted less than 2 MW/m^2. To deal with the heat over 40 MW, the pumped limiter has to be contoured so that the heat is uniformly distributed on the limiter surface. It will be discussed later.

Particles in scrape-off layer diffuse perpendicular to the magnetic flux surface and also move along the magnetic field line. The scrape-off layer width around the main plasma could be determined by the one on the midplane, because the minimum width in the scrape-off layer appears there.

The mean scrape-off layer width on the midplane is assumed to be[4]

$$
\begin{aligned}
\delta_P &= \sqrt{D_\perp \tau_{/\!/}} \quad , \\
D_\perp &= C_D D_B \quad , \\
D_B &= \frac{1}{16} \frac{\bar{T}_{eb}}{B_T} \quad , \\
\tau_{/\!/} &= \frac{L}{v_{/\!/}} \quad , \\
L &= 2\pi R q \quad ,
\end{aligned}
\tag{1}
$$

$$v_{//} = C_s v_s \quad ,$$

$$v_s = \sqrt{\frac{e \bar{T}_{eb}}{M_i}} \quad .$$

Notations are conventional and no details are touched on. In Eq.(1), $D_\perp$ is the perpendicular diffusion coefficient that is assumed to be the Bohm's type. $v_{//}$ is the mean drift velocity parallel to magnetic field line, that is assumed to be directly proprtional to the sound velocity v_s. The unknown multiplication facotrs C_D and C_s in Eq.(1) have been investigated in DIVA experiments[5]. Here, $C_D/C_s = 1$ is assumed in the following analysis.

The scrape-off plasma temperature is restricted by the sheath potential formed in front of the limiter surface. The following relation on the limiter surface between the particle flux $\Gamma(\xi)$ and heat flux $q(\xi)$ must be satisfied:[6]

$$q(\xi) = \gamma T_{eb}(\xi) \Gamma(\xi) \quad , \tag{2}$$

where γ is the heat transmission coefficient in the sheath region, and $T_{eb}(\xi)$ is the scrape-off plasma temperature. The total heat flux Q and total particle flux I therefore obey the following average equation obtained by integrating Eq.(2):

$$Q = \gamma \bar{T}_{eb} I \quad . \tag{3}$$

The average scrape-off plasma temperature T_{eb} is determined from Eq.(3) for the given total fluxes Q and I.

The heat transmission coefficient is calculated by the Hobbs' formula[6] including secondary electron emission effect. The heat transmission coefficient γ is a function of the scrape-off plasma temperature due to the secondary electron emission. The scrape-off plasma temperature is determined consistently with this temperature

dependence of γ.[7] For carbon limiter, we obtained $\bar{T}_{eb}$ = 130 eV using both the INTOR plasma parameters shown in Table 1 and the secondary electron emission coefficient for the electron impact observed in experiment[8]. Then δ_p = 4 cm is obtained from Eq.(1).

The particle flux distribution on the midplane of plasma is assumed to be

$$\Gamma_M(x) = D_M \exp\left(-\frac{x}{\delta_p}\right) \quad , \qquad D_M = \frac{I}{2\pi R_M \delta_p} \quad , \tag{4}$$

where x is the distance from the plasma surface on the midplane and δ_p is given by Eq.(1).

The particle flux parallel to the magnetic flux surface at a given point ξ is obtained from the following relation, taking into account the expansion of scrape-off layer,

$$\Gamma(\xi) = \frac{R_M}{R}\frac{dx}{d\xi}\Gamma_M(x) \quad , \qquad \frac{dx}{d\xi} = \frac{R}{R_M}\frac{B_p}{B_{pM}} \quad , \tag{5}$$

Here, B_{pM} is the poloidal magnetic field at the point x on the midplane of plasma and B_p is the poloidal magnetic field at the given point. R_M is the radial coordinate of the plasma outer surface on the midpane.

Considering that equal amounts of the particle flux go to the inboard and outboard of the limiter, we obtain

$$\Gamma(R) = \frac{1}{2} D_M \frac{B_M}{B_{pM}} \exp\left[-\frac{X(R)}{\delta_p}\right] \quad , \tag{6}$$

where x(R) is the midplane distance from the plasma surface to the given magnetic surface that intersect the limiter surface at a radial coordinate R. The function x(R) is determined by two points x and R

that are on the same magnetic surface calculated by the magnetic surface analysis program[9].

The heat flux distribution is also evaluated in a similar way:

$$q_L(R) = \frac{1}{2} C_M \frac{B_p}{B_{pM}} \exp\left[- \frac{x(R)}{\delta_E} \right] ,$$

$$C_M = \frac{Q}{2\pi R_M \delta_E} . \qquad (7)$$

The e-folding distance δ_E for the heat flux distribution is not so obvious as that for the particle flux distribution. In this analysis, the temperature distribution is assumed to have the same e-folding distance as the particle flux distribution. Consequently the heat flux e-folding distance δ_E becomes a half width of δ_p since the heat flux may be proportional to product of the temperature and particle flux[10]. The scrape-off layer parameters are shown in Table 2.

The particle flux $\Gamma_L(R)$ and heat flux $q_L(R)$ represent the fluxes parallel to the magnetic flux surface, while the particle and heat fluxes normal to the limiter surface are given by $\Gamma_L \sin\theta$ and $q_L \sin\theta$, where θ is the angle between the magnetic flux surface and limiter surface.

The heat flux distributions $q_L \sin\theta$ calculated by Eq.(7) are shown in Fig.2(a) and (b) both for the T-type and N-type pumped limiters, respectively. The maximum heat flux less than the tolerable value $2MW/m^2$ can be attained with the total heat flux, about Q = 40 MW for the both types of pumped limiters. Therefore, the large fraction, about 60% of the α-heating power (120 MW) must be radiated on the entire first-wall before reaching the limiter surface by the charged particle transport. The transported particle flux distributions calculated by Eq.(6) are shown in Figs.3(a) and (b) for the both types of pumped

limiters. It should be noted that the maxima of heat and particle fluxes are slightly higher for the T-type pumped limiter than the N-type one.

4. α-particle exhaust

The charged particles entering the limiter slot are neutralized and pumped out through the exhausting duct or return back to the main plasma. The transmission probability η is defined as probability for the charged particle entering the limiter slot to be neutralized and pumped out through the exhausting duct. In this chapter, the transmission probability and pumping speed necessary for α-particle exhaust are calculated by the divertor conductance calculation program (DICON), which traces particle trajectories using the Monte Carlo simulation method for neutral particle transport[11].

The α-particle transmission probability η_α required to maintain the α-particle concentration in its allowable value, n_α/n_i, is given by the following equation derived from the particle balance equation for α-particles:

$$\eta_\alpha = \frac{1}{f_{slot}} \frac{J_\alpha}{I} \left(\frac{n_\alpha}{n_i} \right)^{-1} , \tag{8}$$

where J_α is the α-particle production rate due to D-T reaction, I is the total ion flux flowing out of the main plasma and f_{slot} is the rate for the particle flux entering the limiter slot. The program DICON directly yields the relation between the α-particle transmission probability and the pumping fraction f_{pump} which is the rate for the neutral particles entering the exhausting duct entrance to be pumped out. Furthermore, the effective pumping speed C_d is related to the pumping fraction by the following conductance formula:

$$C_d = C_0 \frac{f_{pump}}{1 - f_{pump}} , \tag{9}$$

where C_0 is the conductance for the exhausting duct entrance.

The application results of the formalism described here are shown

in Table 3 for the T-type and N-type pumped limiters, where the allowable α-particle concentration 5% is assumed. The η_α-f_{pump} curves are shown in Fig. 4. It should be noted that the effective pumping speed C_d for the N-type pumped limiter is four times larger than that for the T-type pumped limiter.

5. Limiter material

The plasma directly contact with the pumped limiter would be seriously contaminated by the large amount of impurities emitted by the charged particle sputtering of the limiter plate. On the other hand, it is well-known that the scrape-off layer plasma could prevent the impurities released from the limiter or first-wall from flowing into the main plasma.[12),13)] Hereafter, the rate for the released impurity to be shielded from going into the main plasma is called as the impurity shielding efficiency. In this section, the impurity shielding efficiency required for the scrape-off layer to keep the impurity concentration less than its permissible level is calculated by the point model of plasma. It helpes to judge which candidate materials are suitable for the limiter surface.

The impurity concentration is evaluated by the following point model equation of plasma:

$$\frac{dn_Z}{dt} = R_n(1-\zeta_L)(\bar{S}_{DL}\, f_D + \bar{S}_{TL}\, f_T + S_{\alpha L}\, f_\alpha)\,\frac{n_i}{\tau_p} + (1-\zeta_w)(\bar{S}_{DW}\, f_D + \bar{S}_{TW}\, f_T)\,\frac{\varepsilon}{1-\varepsilon}\,\frac{n_i}{\tau_p} + \{R_n\,(1-\zeta_L)\,\bar{S}_{ZL} - (1-R_Z)\}\, f_Z\,\frac{\tau_p}{\tau_Z}\,\frac{n_i}{\tau_p} \quad , \tag{10}$$

where ζ_L or ζ_W is the impurity shielding efficiency for impurities released from the limiter plate or first wall, respectively.

The first term in right-hand side of Eq.(10) represents the accumulation rate of impurities released from the limiter plate, where $\bar{S}_{DL}$, $\bar{S}_{TL}$ and $\bar{S}_{\alpha L}$ are the average sputtering coefficients of the limiter plate for D, T and α ion impact, and f_D, f_T and f_α are the fractions of D, T and α ions in the main plasma. R_n is a fraction for the ions flowing

out of the main plasma to collide with the limiter front surface. The second term in right-hand side of Eq.(10) represents the accumulation rate of impurities released from the first-wall, where $\bar{S}_{DW}$ and $\bar{S}_{TW}$ are the average sputtering coefficients of the first-wall for D and T ion impact, and ε is the escaping ratio of the charge exchange neutral. The last term in Eq.(10) describes the accumulation rate of the self-sputtered impurities and evacuating rate of impurities, where $\bar{S}_{ZL}$ is the average self-sputtering coefficient, f_Z is the impurity fraction in plasma, R_Z is the recycling rate for impurities and τ_Z is the impurity confinement time in plasma.

All the physical sputtering coefficients including the self-sputtering coefficients are calculated from the Smith's formula.[14] As for the chemical sputtering coefficients for carbon, the experimental data for hydrogen impact measured at 500°C by Yamada, et al. is used.[15] The ion impact energy is calculated by

$$E_I = T_{eb} \left(\frac{3}{2} + \alpha \langle Z_I \rangle \right) \quad , \tag{11}$$

where α is the sheath potential in T_{eb}-unit and $\langle Z_I \rangle$ is the mean charge of the impinging ion which is estimated by assuming coronal equilibrium[16] in the scrape-off layer.

The impurity recycling coefficient is calculated based on the assumptions that all the impurity ions entering the limiter slot are evacuated and the impurity ions hitting the limiter front surface are reflected or absorbed according to the reflection coefficient obtained by Lindhard.[17]

The impurity shielding efficiency ξ_L required to keep the impurity concentration in its permissible level is calculated by taking the left-hand side of eq.(10) equal to zero and solving the resulting equation with respect to ζ_L. The calculated results are shown in Fig. 5

for the candidate materials such as Mo, C, SiC and TiC. The impurity permissible levels are assumed in this analysis, 0.01% for W, 0.05% for Mo, 2% for C and 0.5% for SiC and TiC. In addition, the charge exchange neutral energy is taken equal to the boundary temperature and $\zeta_W = 0.9$, $\varepsilon = 0.5$ and $\tau_Z/\tau_p = 1$ are tentatively used. The calculated result for carbon in Fig. 5(a) is obtained by using only the physical sputtering coefficients. Inclusion of the chemical sputtering coefficient in addition to the physical one yields the results shown in Fig. 5(b).

It can be seen from Fig. 5(a) that the application of tungsten and molybdenum to INTOR limiter require the very high shielding efficiency for the scrape-off layer. As for SiC and TiC, the relatively high shielding efficiency $0.8 \sim 0.9$ is necessary at the reference scrape-off plasma temperature 130 eV. However this value of the shielding efficiency is still in the realizable range. At the lower scrape-off plasma temperature, about 40 eV, the required shielding efficiency is moderate value, about 0.5. The boundary plasma cooling due to the radiation loss by the released impurity itself is possible to reduce the scrape-off plasma temperature, probably less than 40 eV. The further studies in the boundary plasma cooling will be needed to ensure the applicability of SiC and TiC. On the other hand, it is proved from Fig. 5(b) that the boundary cooling is less effective for carbon limiter because the chemical sputtering is the most dominant process of the impurity production and more weakly dependent on the scrape-off plasma temperature than the physical one. The control of the limiter surface temperature could probably reduce the impurity production because the chemical sputtering is very small in temperature range except for $300°C \sim 700°C$.

Finally the erossion thickness of the limiter surface is estimated

by the following equation for the both types of the pumped limiters:

$$d(R) = \{S_{DL}(R)\ f_D + S_{TL}(R)\ f_T + S_{\alpha L}\ f_\alpha + S_{ZL}(R)\ f_Z\}$$
$$\Gamma_L(R)\ \sin\theta \cdot \left(\frac{A}{N\rho}\right)\ t \cdot D \cdot A_V \quad , \tag{12}$$

where A is the atomic weight of limiter material, ρ the density of wall material, N the Avogadro's number, t the time of irradiation, D the duty cycle and A_V the availability. The ion impact energy E_I as well as the scrape-off plasma temperature T_{eb} are changed with the total heat flux Q. The calculated results of the carbon erosion thickness at the maximum particle flux are shown in Fig. 6 as a function of the total heat flux, where D = 0.5 and A_V = 0.25 are assumed. It is shown in Fig. 6 that the maximum erosion is about 2 cm/year. The exchange cycle of the limiter plate should be discussed in future study taking the thermal-hydraulic and stress analyses and the redeposition of sputtered materials into consideration.

6. Preliminary studies on curved limiter configuration accepting larger heat

It was presented in the previous chapters that the maximum total permissible heat flux to the flat-type limiter is restricted under around 40 MW, when the maximum acceptable heat flux density is limited less than 2 MW/m^2. The INTOR standard design specification, however, says that 80 MW thermal power of the α-heating power (124 MW) is transfered to the limiter. Therefore, the workable pumped limiter consistent with the INTOR standard specifications could be designed by contouring the limiter receiving uniform heat flux distribution. Here, as a first step, the limiters with different curvatures are investigated.

The heat and particle fluxes are calculated by the same method described in the previous chapter. Circularly curved limiter surfaces of two curvatures, $\rho = 1.5$ m and $\rho = 3$ m, are analyzed for the toal heat flux Q = 80 MW and the energy scrape-off width $\delta_E = 1.5$ cm. The results shown in Fig. 7 tell, needless to say, that the maximum heat flux amounts to 4 MW/m^2 for the flat-type limiter, which imposes very severe conditions on the limiter design. It also indicates that the maximum heat flux less than 2 MW/m^2 could be attained only with the curvature smaller than 1.5 m. It is feared, however, that the heat flux distribution would be very sensitive to the horizontal displacement of the plasma, because of the adjacency of the limiter surface to the plasma surface in the circularly curved limiter.

The contoured limiter, suffering the arbitrary heat distribution on its surface, might be necessary for the more developed limiter design. The desirable heat distribution depends on the erosion and redeposition of the limiter material and the thermal hydraulics and thermal stress analysis. The limiter design including such considerations is now underway and will be reported in near future.

7. Sensitivity of the limiter leading edge

The most severe problem in the T-type pumped limiter would be the sensitivity of the heat and particle loads at the limiter leading edge. Figure 8 shows the changes of heat and particle fluxes at the limiter leading edge, and that of the pumping speed, corresponding to the horizontal shift of plasma center, ΔR_p, as well as to the scrape-off layer parameters, δ_E and δ_p. In the figure, the dots stand for the baseline values, $q_{edge} = 3$ MW/m^2, $\Gamma_{edge} = 7.5 \times 10^{21}$ 1/m^{2}s and $C_d = 2.5 \times 10^5$ ℓ/s. The required margins are $\Delta q_{edge} = 1$ MW/m^2, $\Delta\Gamma_{edge} = 1.5 \times 10^{21}$ 1/m^{2}s and $\Delta C_d = 10^5$ ℓ/s as to the horizontal shift, $\Delta R_p = \pm 5$ cm, and $\Delta q_{edge} = 1$ MW/m^2, $\Delta\Gamma_{edge} = 0.5 \times 10^{21}$ 1/m^{2}s and $\Delta C_d = 3 \times 10^5$ ℓ/s as to the changes in the scrape-off widths, $\Delta\delta_E = \pm 0.5$ cm and $\Delta\delta_p = \pm 1$ cm.

8. Conclusions

The two typical limiter configurations were proposed and discussed for the toroidal belt-type pumped limiter located at the bottom of plasma in INTOR. In the first configuration (T-type pumped limiter), the limiter plate is set up tangential to the outermost magnetic flux surface of plasma. In the second configuration (N-type pumped limiter), the limiter plate is inserted near the null point of the poloidal magnetic field.

The conditions imposed by the heat flux and particle flux on the limiter plates are almost similar both for the T-type and N-type pumped limiters. It becomes clear that the significant fraction of the α-heating power, larger than 60%, must be removed by something like the radiation in order to suppress the maximum heat flux onto the limiter surface less than 2 MW/m^2. The effective pumping speed required for the main exhausting system is four times larger for the N-type pumped limiter than for the T-type one. The N-type pumped limiter seems to suffer from the rather severe requirement, 6.6×10^5 ℓ/s, in designing the actual exhausting system. Some effects to ease the pumping speed requirement could, however, be expected, such as the density enhancement of the scrape-off plasma in the limiter slot, that should be discussed in the future study.

The limiter candidate materials are discussed on the basis of the impurity accumulation analysis by using the point model of plasma. It is found that for the SiC and TiC limiters, the boundary cooling of plasma, e.g., less than 40 eV, could suppress the impurity concentration less than its permissible level, while for the carbon limiter, the control of the limiter temperature instead of the plasma boundary cooling is effective in reducing the impurity production. In order

to ensure the applicability of the SiC and TiC limiters, the further studies are necessary for the plasma boundary cooling due to radiation loss by the released impurity itself.

The preliminary study for accepting the total heat of 80 MW indicates that the circularly curved limiter with its curvature of less than 1.5 m could make the peak heat flux less than 2 MW/m^2. The sensitivity of the heat and particle load on the limiter edge and the pumping speed is analyzed changing the scrape-off layer width and the plasma major radius, and it is found that the limiter design should be performed to be consistent with the accuracy of the plasma positioning. The allowable variations of the plasma parameters will be discussed in detail in the future.

Acknowledgement

The authers are indebted to Drs. Yasuhiko Iso, Ken Tomabechi, and Masaji Yoshikawa for continuous encouragement. They also thank Dr. Toru Hiraoka for useful discussions.

to ensure the applicability of the SiC and TiC limiters, the further studies are necessary for the plasma boundary cooling due to radiation loss by the released impurity itself.

The preliminary study for accepting the total heat of 80 MW indicates that the circularly curved limiter with its curvature of less than 1.5 m could make the peak heat flux less than 2 MW/m^2. The sensitivity of the heat and particle load on the limiter edge and the pumping speed is analyzed changing the scrape-off layer width and the plasma major radius, and it is found that the limiter design should be performed to be consistent with the accuracy of the plasma positioning. The allowable variations of the plasma parameters will be discussed in detail in the future.

Acknowledgement

The authers are indebted to Drs. Yasuhiko Iso, Ken Tomabechi, and Masaji Yoshikawa for continuous encouragement. They also thank Dr. Toru Hiraoka for useful discussions.

References

1) INTOR Group, Report "International Tokamak Reactor: Phase One", IAEA, Vienna, 1982.

2) Tomabechi, K., et al., Third IAEA Technical Committee Meeing and Workshop on Fusion Reactor Design and Technology (Tokyo) 1981.

3) Iida, H., et al., JAERI-M 8944 (1980).

4) Shimomura, Y., et al., JAERI-M 7457 (1977).

5) Kimura, H., et al., Nucl. Fusion 1980 (1978), 1195.

6) Hobbs, G.D. and Wesson, J.A., Plasma Physics 9 (1967), 85.

7) Saito, S., et al., JAERI-M 82-011 (1982).

8) Barnet, C.F., et al., ORNL-5207 (1977).

9) Shinya, K. and Ninomiya, H., JAERI-M 9278 (1981).

10) Baker, C.C., et al., "STARFIRE, a commercial tokamak power plant design"

11) Seki, Y., et al., Nucl. Fusion 70 (1980), 1213.

12) Kishimoto, H., tani, K. and Nakamura, H., JAERI-M 9783 (1981).

13) Sengoku, S., et al., Nucl. Fusion 19 (1979), 1237.

14) Smith, D.L., J. Nucl. Mater. 75 (1978), 20.

15) Yamada, R., et al., J. Nucl. Mater. 95 (1980), 278.

16) Breton, C., et al., EUR-CEA-FC-948.

17) Lindhard, J., Scharff, M. and Schiott, H., Mat. Fys. Medd. 33 14 (1963), 39.

Table 1 Major plasma parameters for INTOR

major radius, R(m)	5.3
minor radius, a(m)	1.2
elongation , κ	1.6
average temperature, T_p(keV)	10
average density , n_p(m^{-3})	1.4×10^{20}
toroidal field , B_T(T)	5.5
safety factor , q_ψ	2.1
fusion power , P_T(MW)	620
toroidal beta , β_T(%)	5.6
poloidal beta , β_p	2.6
plasma current , I_p(MA)	6.4
energy confinement time, τ_E(s)	1.4
particle confinement time, τ_p(s)	0.2

Table 2 Scrape-off layer plasma parameters for INTOR

transport heat load, Q(MW)	40
scrape-off plasma temperature, $\bar{T}_{eb}$ (cV)	130
particle flux e-folding distance, δ_p (cm)	4
heat flux e-folding distance, δ_E (cm)	2

Table 3 Comparison of the exhausting characteristics for the proposed pumped limiters

	T-type pumped limiter	N-type pumped limiter
flux fraction entering the limiter slot, f_{slot}	0.21	0.5
transmission probability, η_α	0.13	0.053
pumping fraction, f_{pump}	0.012	0.062
conductance for the duct entrance, C_o (ℓ/s)	1.2×10^7	1.0×10^7
effective pumping speed, C_d (ℓ/s)	1.5×10^5	6.6×10^5

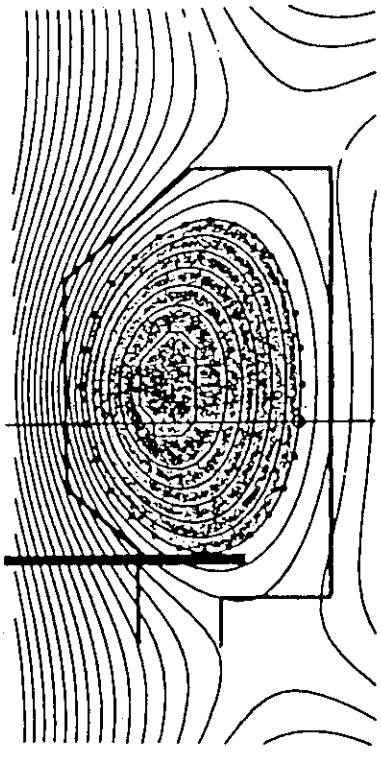

(a) T-TYPE PUMPED LIMITER

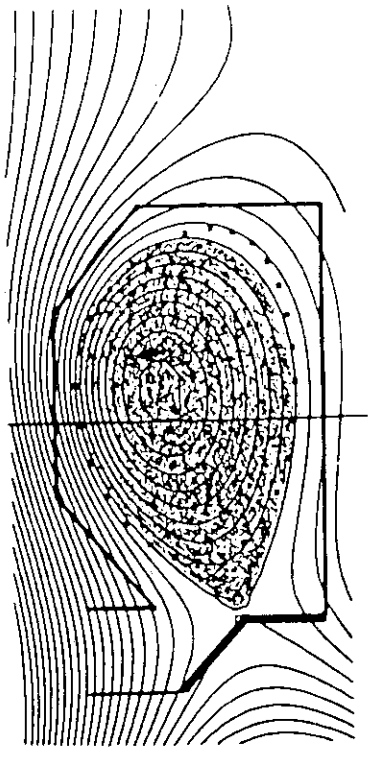

(b) N-TYPE PUMPED LIMITER

Fig. 1 Poloidal cross section of the proposed pumped limiter configurations.

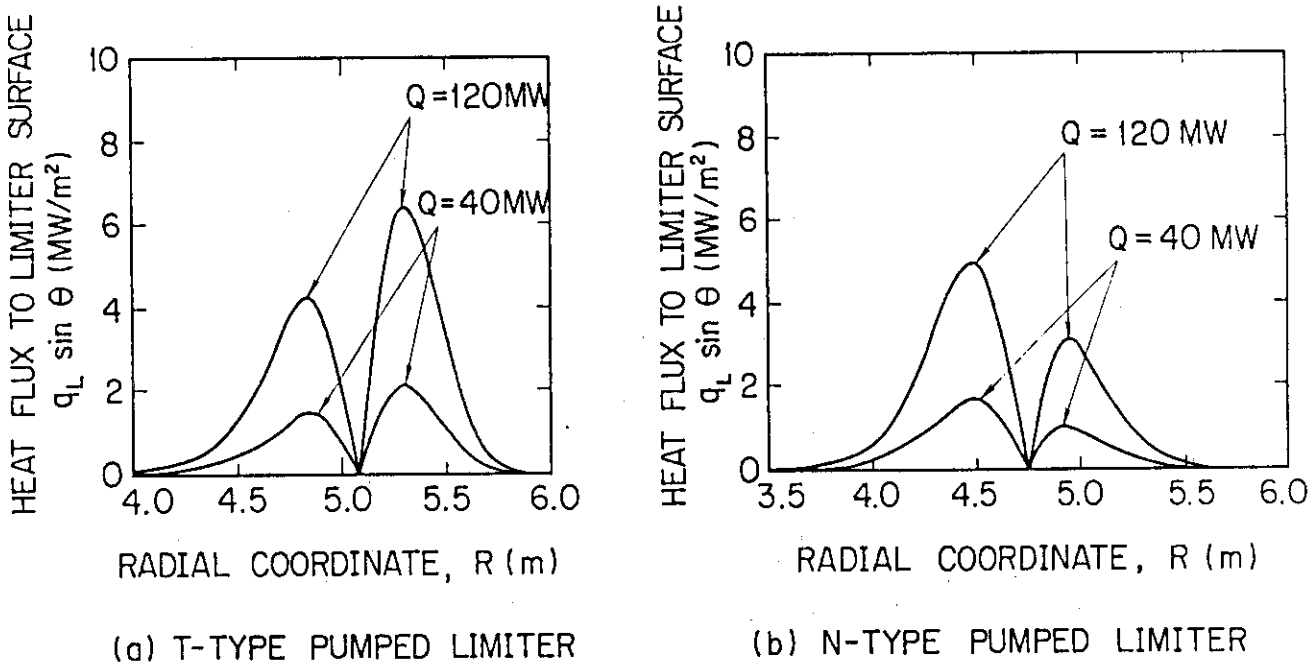

Fig. 2 Calculated transport heat fluxes to the proposed pumped limiters. for the total heat flux Q = 120 MW and Q = 40 MW.

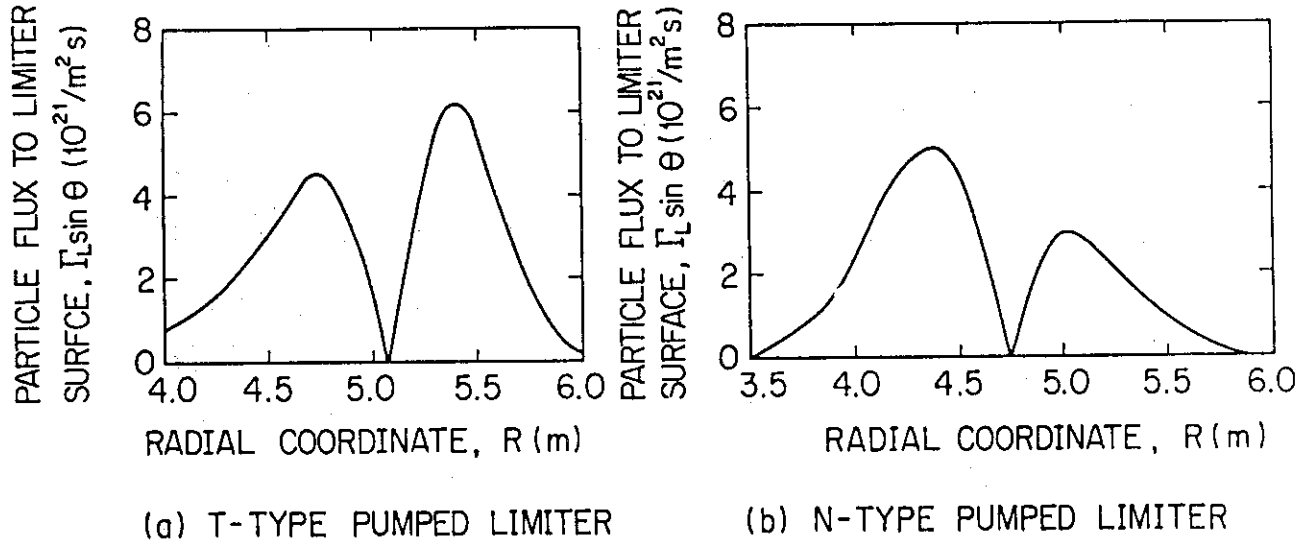

Fig. 3 Cacluated transport particle fluxes to the proposed pumped limiters.

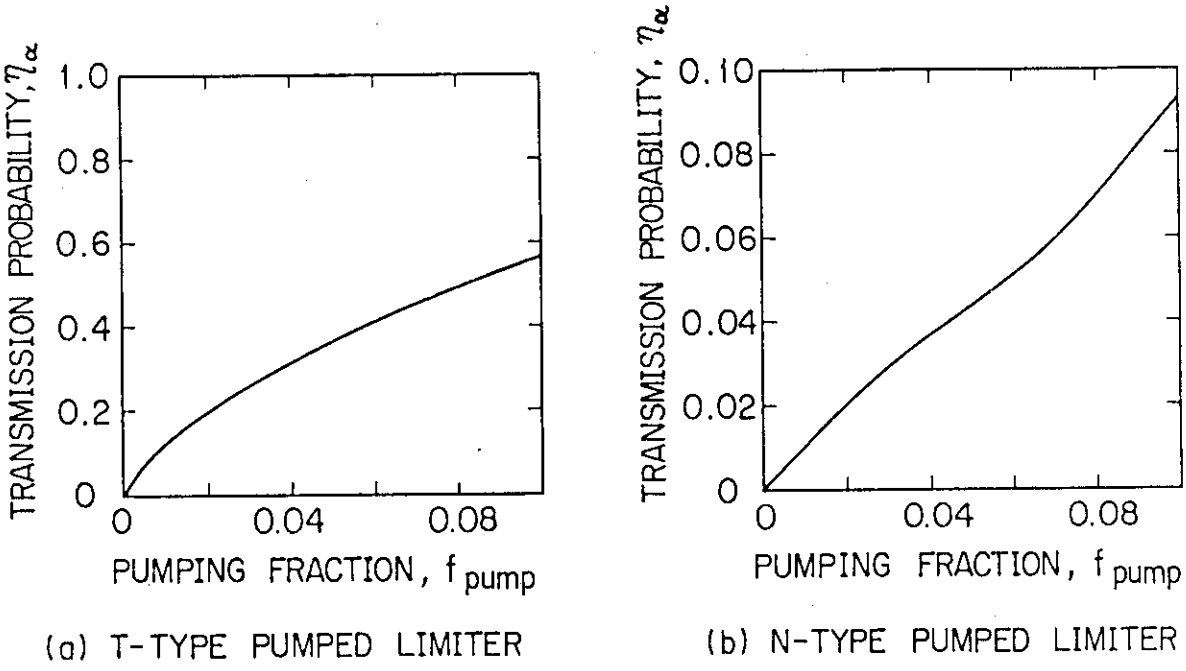

Fig. 4 α-particle transimission probabilities for the proposed pumped limiters calculated by the Monte Carlo simulation for the neutral particle transport. The transimission probability is the probability for the charged particle entering the limiter slot to be neutralized and pumped out.

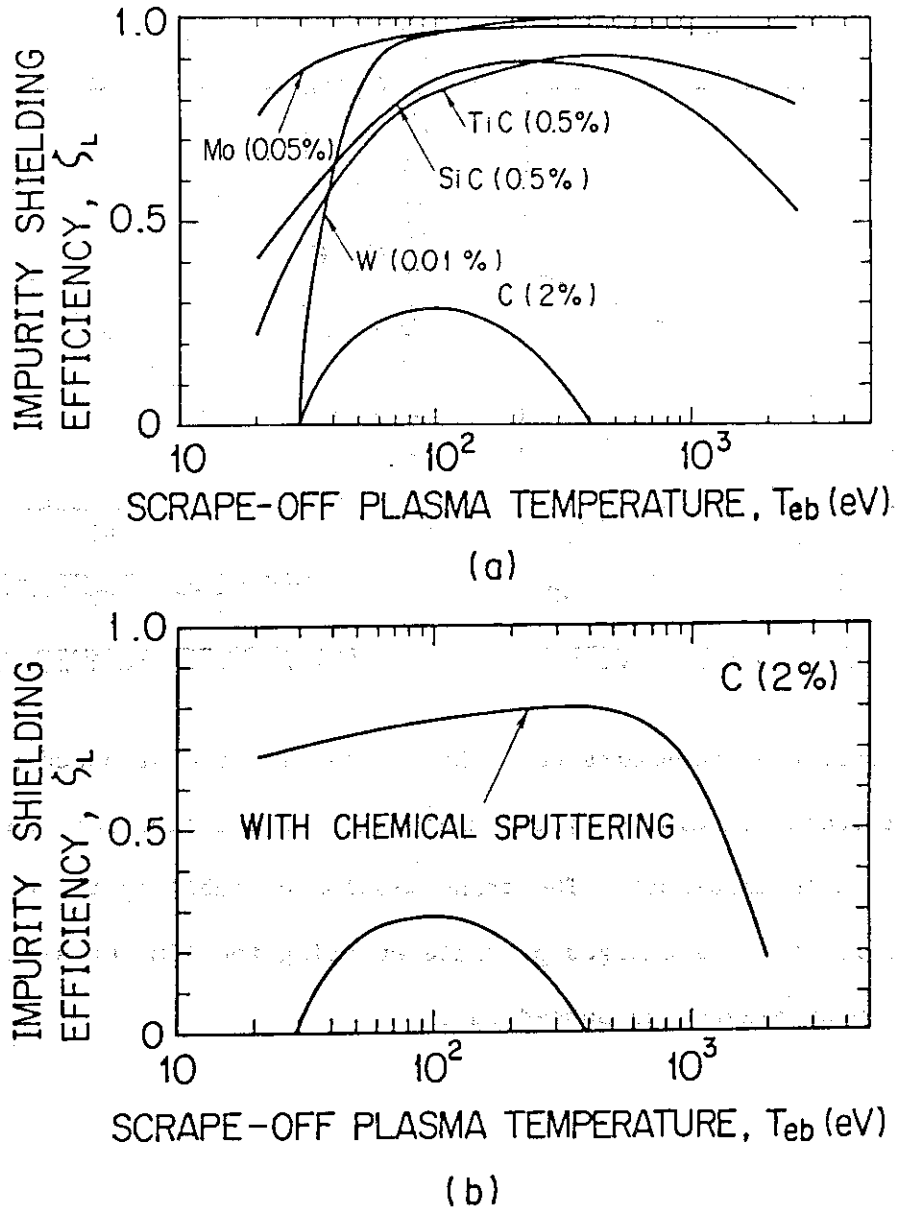

Fig. 5 Required impurity shielding efficiency in the scrape-off layer of plasma: (a) for the several candidate materials such as tungsten (W), molybdenum (Mo), carbon (C), and SiC and TiC, (The result for carbon is obtained by using only the physical sputtering coefficients from Smith's formula.) (b) for carbon which is obtained including the chemical sputtering effect based on the JAERI experimental data.

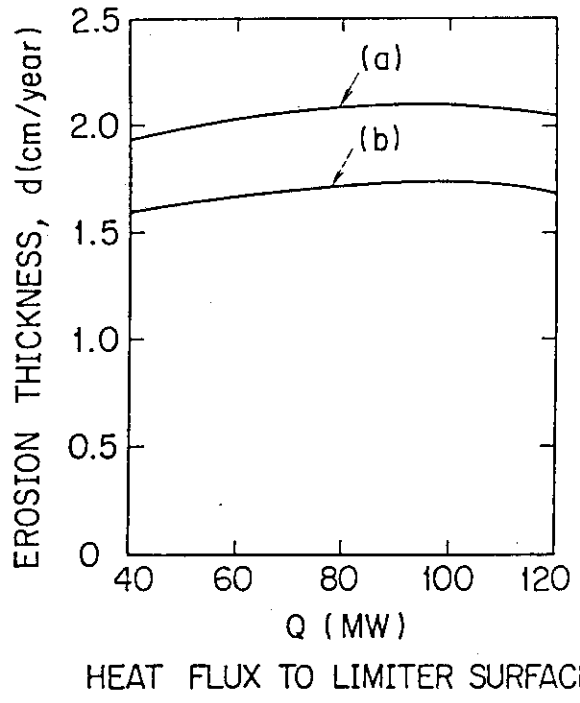

Fig. 6 Calculated erosion thickness of the carbon limiter at the maximum particle flux for the proposed pumped limiter: (a) T-type pumped limiter, and (b) N-type pumped limiter.

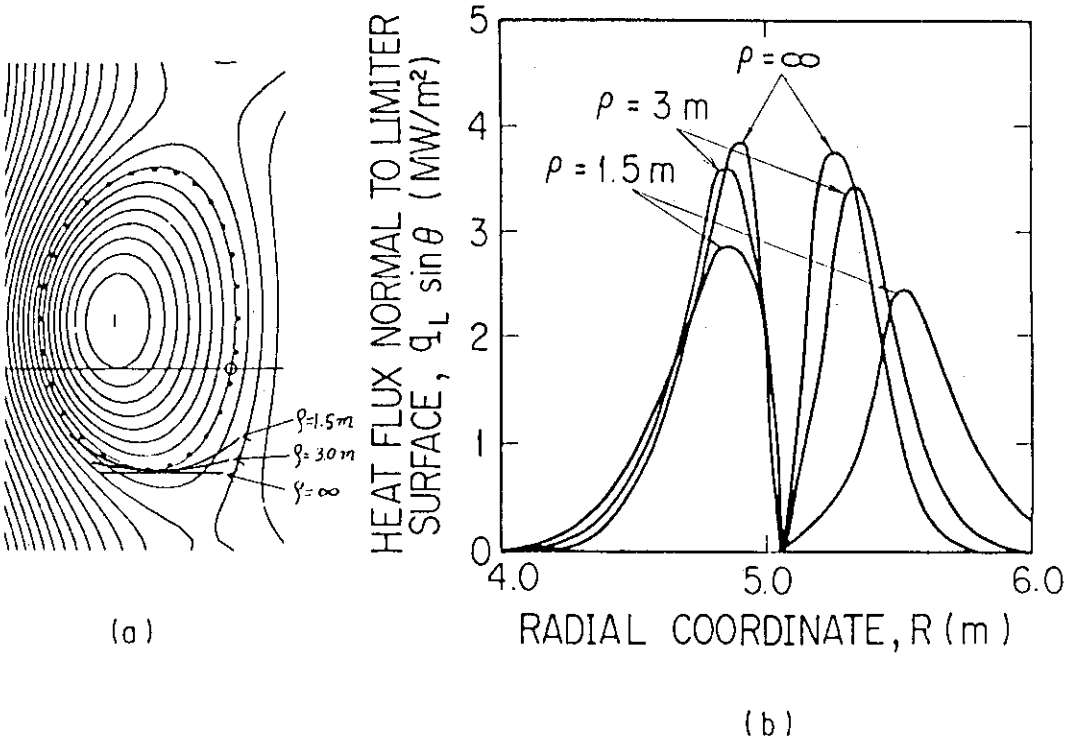

Fig. 7 Heat flux distributions on the circularly curved limiter: (a) limiter configurations with different curvatures, ρ, (b) heat flux distributions corresponding to the different curvatures, ρ.

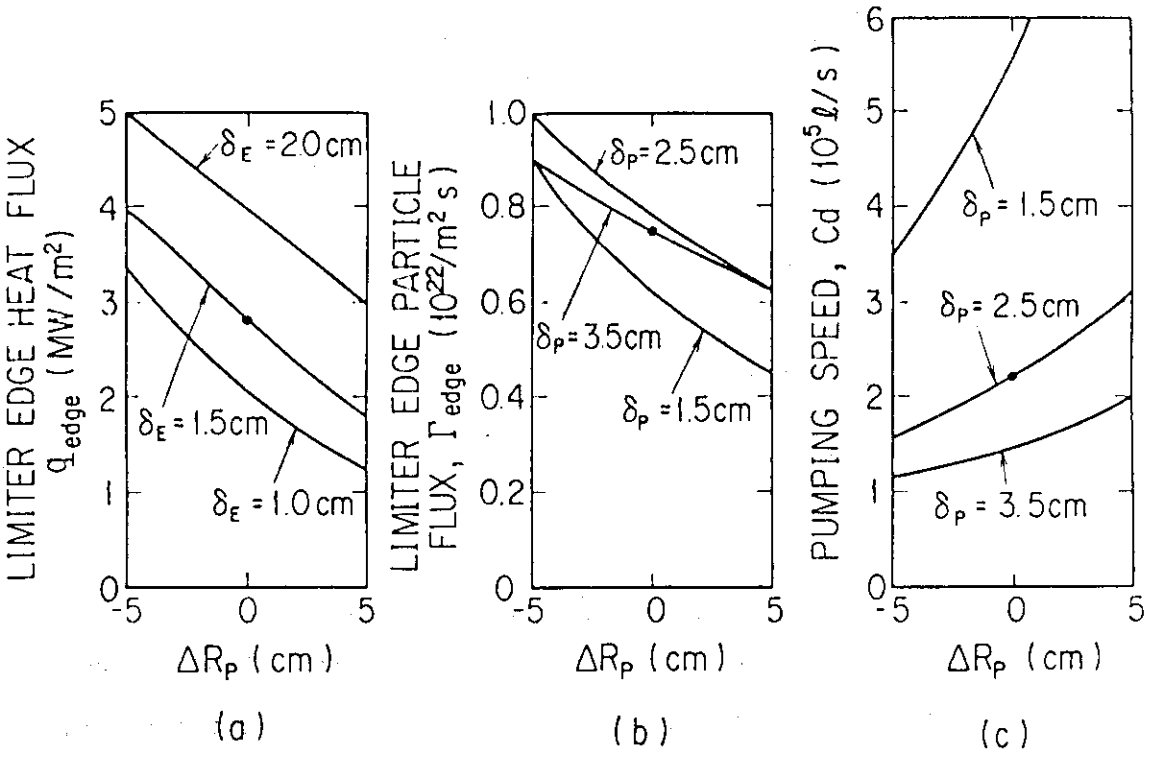

Fig. 8 The sensitivity of the heat and particle loads at the limiter leading edge, and that of the pumping speed: (a) the heat flux at the leading edge as a function of the plasma outward shift, ΔR_p, where the heat flux e-folding distance δ_E is changed, (b) the particle flux at the leading edge as a function of ΔR_p where the particle flux e-folding distance δ_p is changed, (c) the required pumping speed as a function of ΔR_p where δ_p is changed.